COMMUNICATION

Check for updates

Crystallization-induced emission from F-doped carbon dots†

Tingxuan Guo,‡[a] Gaixia Yang,‡[a] Yan Li, ID *[a] Can Liu, ID [a] Fulin Yang,[a] Defa Hou, ID [a] Hao Sun,[a] Yunwu Zheng, ID [a] Xu Lin ID *[a] and Lanxiang Liu*[b]

Herein, F-doped CDs with bright red SSF were synthesized by a solvothermal method using trifluoroethanol as the solvent and *m*-hydroxybenzaldehyde as the carbon source. Strong F–F interactions are vital for inducing crystallization, and solid luminescence is achieved by blocking the nonradiative energy dissipation pathways of crystalline organizations.

Carbon dots (CDs),[1,2] due to their excellent optical properties, low toxicity, good biocompatibility, environmental friendliness, and ease of preparation, have shown promise in various fields.[3–5] However, high-performing CDs often suffer from severe aggregation-driven quenching (ACQ) in the solid state due to the predominance of nonradiative energy dissipation pathways, which limits their commercial applicability.[6,7] In recent years, researchers have used various strategies to circumvent ACQ caused by fluorescence resonance energy transfer (FRET) and direct π–π interactions between fluorescence sources.[8–12] The main methods include dispersing CDs into other matrix materials to form composite materials, introducing long-chain alkyl groups to increase steric hindrance, and regulating surface functional group structures and aggregate-induced emission.[13–17] Among these methods, crystallization-induced emission (CIE) is an important method for avoiding fluorescence quenching.[18] The CIE properties arise due to intermolecular interactions in the crystal structure that result in locking of the ground state molecular geometry and blocking relaxation from the excited state.[19,20] To achieve CIE, additional strong interactions, such as hydrogen bonding, must be introduced into carbon dots to increase crystallinity.[21,22]

[a]National Joint Engineering Research Center for Highly-Efficient Utilization Technology of Forestry Resources, Southwest Forestry University, 300 Bailong Road, Kunming 650224, Yunnan, China

[b]Institute of Highland Forest Science, Chinese Academy of Forestry, National Forestry and Grassland Administration, Kunming 650233, China

† Electronic supplementary information (ESI) available. See DOI: https://doi.org/10.1039/d4na00206g

‡ These authors contributed equally to this work.

However, as electron acceptors, hydrogen bonding moieties often affect excited-state electrons, affecting efficiency.[23]

The replacement of hydrogen with fluorine leads to changes in the physical and chemical properties of compounds. It has been proven that the fluorination of alkyl groups in proteins affects protein folding through F⋯F interactions.[24] In addition, fluorination of an organic compound can significantly enhance intermolecular interactions and crystal stability.[25] Although F⋯F interactions are considered weak and are weaker than hydrogen bonding interactions, they play an important role in molecular assembly and crystal engineering.[26] Due to the strong electronegativity of F atoms and the highly polarized nature of C–F bonds, F doping has become an effective strategy for inducing solid-state fluorescence (SSF) by adjusting the surface electronic state and interactions of CDs.[27,28] Unfortunately, all the reported F-doped SSF carbon dots exhibit varying degrees of ACQ, resulting in lower fluorescence efficiency in the solid state, although they exhibit bright fluorescence in the solution state.[29–33]

Herein, we report the synthesis of a novel kind of red-emissive SSF-CD ($\lambda_{em} = 640$ nm) that is prepared by F-doping *via* a facile solvothermal approach (Fig. 1). The prepared F-CDs exhibit crystallinity, and their red fluorescence efficiency in the solid state is similar to that in solution. However, a control sample without F-doping (H-CDs) shows no SSF. The XRD results show that F-doping leads to the formation of crystal structures in F-CDs, and this crystal conformation prevents compact π–π packing. The strong interactions between F atoms in the F-CDs allowed for the preparation of white LEDs by room-temperature pressing. The results of this study expand on the synthesis strategies available to prepare controlled SSF CDs, which is very important in this emerging field.

As shown in Fig. 1, the F-CDs were synthesized by a simple one-pot solvothermal method at 180 °C using trifluoroethanol as the solvent and *m*-hydroxybenzaldehyde as the carbon source. The precipitate was first removed from the reaction suspension, and then the solvent was removed by rotary evaporation to obtain orange crystals that emitted red fluorescence

Fig. 1 Schematic of the synthesis procedures; optical images of the CDs dispersed in ethanol solution under 365 nm UV light. Schematic diagram of the SSF mechanism model.

under a 365 nm UV lamp. Through scanning electron microscopy (SEM) observations of these crystals, it was found that the F-CDs form a large crystal structure with a thickness of approximately 15.5 μm, while the H-CDs are composed of smaller amorphous structures, indicating that there were strong interactions among the F-CDs (Fig. 2a and b). This crystalline structure was dissolved in ethanol and diluted to 1.0 mg mL^{-1}, after which the sample was observed by TEM, and an aggregated structure of 20–35 nm was still observed (Fig. 2c). The carbon dot solution was further diluted to 0.1 mg mL^{-1}, and discrete carbon dots with an average diameter of 2.0 ± 0.1 nm were observed. In contrast, discrete carbon dots can be observed in the H-CDs at a concentration of 1 mg mL^{-1}, with an average diameter of 3.5 ± 0.2 nm (Fig. 2d). Fig. S1† shows a high-resolution TEM (HR-TEM) image of individual F-CDs and H-CDs, which reveals the high crystallinity of the carbon core.
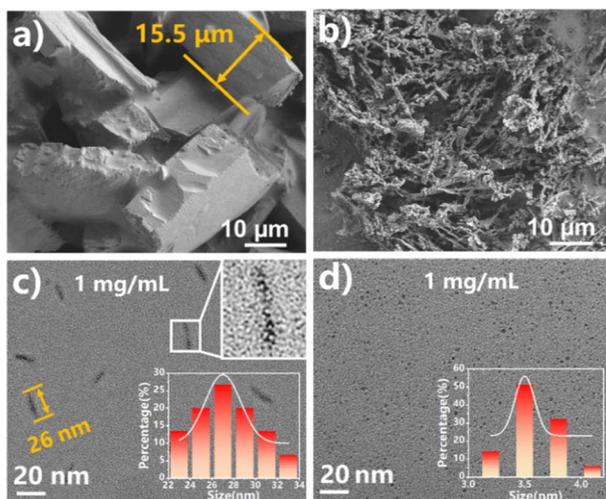
The spacing of the lattice fringe is 0.20 nm, which corresponds to the (100) plane of graphitic carbon.[34]

The geometrical structures of the two types of CDs were analysed *via* X-ray diffraction (XRD) (Fig. 3a). The broad peak at 26.5° in the XRD pattern of the H-CDs corresponds to the (002) facet of graphite and is attributed to amorphous carbon derived from deformations caused by heteroatomic dopants or sp^3 carbon defects in graphitic structures.[35,36] The XRD pattern of the F-CDs shows many sharp diffraction peaks, which confirms the crystal structure.[37] Due to the strong interactions among F atoms, crystallization is induced, circumventing direct face-to-face π–π aggregation between carbon dots, which is likely to be the reason for the solid-state fluorescence phenomenon.

The chemical composition and surface functional groups of the H-CDs and F-CDs were examined by Fourier transform infrared (FT-IR) and X-ray photoelectron spectroscopy (XPS). As shown in Fig. 3b, the FT-IR spectra indicate the presence of O–H (3012–3680 cm^{-1}), C=O (1663 cm^{-1}), and C=C (1570 cm^{-1}) bonds in both samples, but a unique vibrational peak corresponding to the C–F bond (1074 cm^{-1}) is present in the F-CD spectrum.[30,38] In addition, the full-survey XPS spectra (Fig. 3c) confirm the presence of F in the F-CD sample. As shown in Fig. 4d, the H-CDs contain C and O at proportions of 83.2% and 16.8%, respectively, while the F-CDs mainly contain C, O and F at proportions of 78.2%, 18.8% and 3.0%, respectively. In addition, the high-resolution XPS spectrum of C 1s (Fig. 3d) shows four peaks at 284.8, 286.7, 288.5, and 291.2 eV, which can be assigned to C–C/C=C, C–O, C=O and C–F bonds,

Fig. 2 SEM images of the (a) F-CDs and (b) H-CDs. TEM image (inset: the corresponding particle size distribution histogram) of the (c) F-CDs and (d) H-CDs.

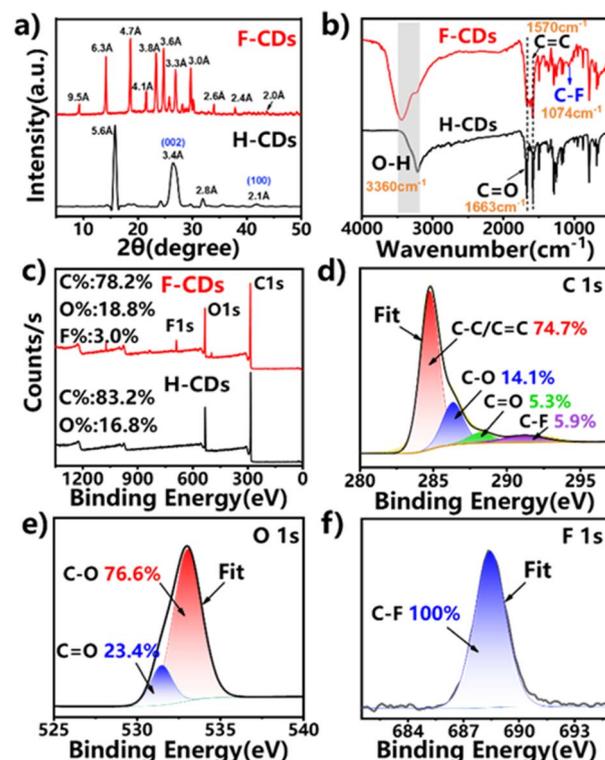**Fig. 3** (a) XRD pattern image, (b) FTIR spectra, (c) XPS survey spectra, and high-resolution (d) C 1s, (e) O 1s, and (f) F 1s spectra of the F-CDs.
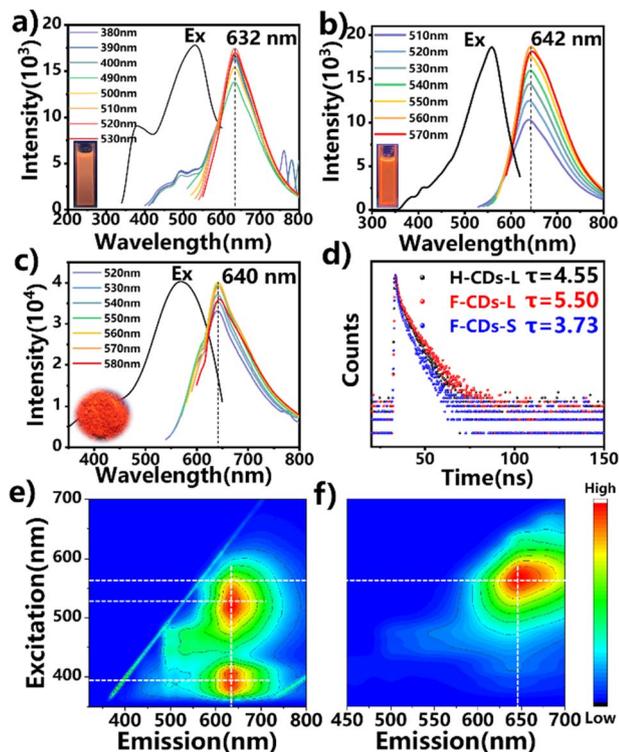
Fig. 4 PL emission spectra of (a) F-CDs-l, (b) H-CDs-l, and (c) F-CDs-s at different excitation wavelengths; (d) photoluminescence decays of H-CDs and F-CDs in ethanol solution and ($c = 0.1$ mg mL^{-1}) in the solid state; 3D PL spectra of (e) F-CDs-l and (f) H-CDs-l.

Table 1 Fluorescence characterization data of F-CDs-L, H-CDs-L, and F-CDs-S

	F-CDs-L	H-CDs-L	F-CDs-S
λ_{ex}	531 nm	550 nm	555 nm
λ_{em}	632 nm	642 nm	640 nm
QYs	30.0%	38.0%	28.0%
τ_{avg}	5.50 ns	4.55 ns	3.73 ns

respectively.[39,40] The O 1s spectrum can be deconvoluted into two peaks at 531.5 and 533.1 eV, ascribed to C=O and C–O, respectively (Fig. 3e).[41] In particular, the high-resolution F 1s spectrum (Fig. 3f) shows a typical signal corresponding to the C–F bond (688.4 eV).[42] The high-resolution C 1s and O 1s XPS spectra of the H-CDs are also shown in Fig. S2.† The above results show that F is successfully doped into F-CDs using trifluoroethanol as the solvent.[43]

The optical properties of the F-CDs and H-CDs in both the solution state and solid-state were investigated. Fig. S3† shows the UV-vis absorption of the solution-state F-CDs, H-CDs and solid-state F-CDs. Both CDs show two main absorption peaks at 254 nm and 317 nm, which can be attributed to the π–π* and n–π* transitions, respectively.[44,45] However, compared to those of the H-CDs, the F-CDs have a broader UV-vis absorption range, which could have occurred because new defects were induced by F-doping.[46] The H-CDs and F-CDs in the solution state emit red fluorescence, and their emission peaks occur at 642 nm and 632 nm, respectively, under UV excitation ($\lambda_{ex} = 365$ nm); both the F-CDs and H-CDs exhibit excitation-independent emission behaviour (Fig. 4a, b and Table 1). Under optimal excitation, the fluorescence quantum yields (QYs) of the F-CDs and H-CDs in ethanol are 30% and 38%, respectively. Due to the influence of the electron-absorbing group of F atoms, the emission peak of the F-CDs is blue-shifted, and the QY is lower than that of the H-CDs. In addition, the time-resolved PL decay data show that the F-CDs have a longer average fluorescence lifetime ($\tau_{avg} = 5.50$

ns) than the H-CDs ($\tau_{avg} = 4.55$ ns) (Fig. 4d).[47] The 3D spectrum shows that both CDs only have red emission centres; the difference is that F-CDs can be excited by two optimal light sources of different wavelengths and then emit light at the same wavelength; that is, F-CDs have two channels for achieving strong fluorescence, which may be related to the new absorption region formed due to F-doping (Fig. 4e and f).[48] In the solid state, the F-CDs exhibit bright red fluorescence with an emission peak at 640 nm and an excitation peak at 560 nm, without excitation dependence (Fig. 4c). Compared with that in the liquid state, the F···F interaction in the solid-state promotes a redshift in the emission peak and prevents fluorescence quenching.[49] In contrast, solid-state H-CD samples did not show any fluorescence under excitation of all different wavelengths.

To investigate the formation process of CDs and their reaction mechanism, we performed time gradient experiments on the synthesized F-CDs (Fig. S6–8†). As the reaction progressed, the normalized PL spectra show that the maximum emission wavelength of the F-CDs slowly redshifted from 420 nm to 632 nm, which indicates that the conjugated structures of the fluorophores in the F-CDs gradually became larger. The F-CD solid powder began to display a fluorescent colour after approximately 3 h and reaches its brightest point after 6 hours. Based on dynamic NMR analysis of F-CDs and our previous research,[50] we believe that the –CH$_2$CF$_3$ group is introduced at the 5-site of *m*-hydroxybenzaldehyde during the reaction (Fig. 5a) and that the F···F interaction supports the crystal structure and prevents strong π–π stacking, blocking the major approach for nonradiative energy dissipation in crystalline aromatic compounds and inducing SSF.[51,52] The unit structure of the fluorescent molecules in the F-CDs might be dyad 4. In addition, the length of the molecule along the long axis of the dyad was approximately 1 nm. The average particle size of the F-CDs as measured by TEM was approximately 2.0 nm, suggesting that the fluorescent molecules were concentrated by as many as four units. After supramolecular aggregation, CDs were formed with a layer spacing of 0.2 nm. This process could enhance photoluminescence by restraining the movement of the fluorescence center, akin to the emission enhancement effect of supramolecular cross-linking.[53–55]

SSF was not observed when *o*-hydroxybenzaldehyde and *p*-hydroxybenzaldehyde were used as the reaction matrix (Fig. S9†). In addition, the CDs obtained under acidic or alkaline conditions also did not exhibit SSF (Fig. S10†), possibly because the acid or base destroyed the reactive sites and –CH$_2$CF$_3$ was not successfully introduced at the 5-site of *m*-
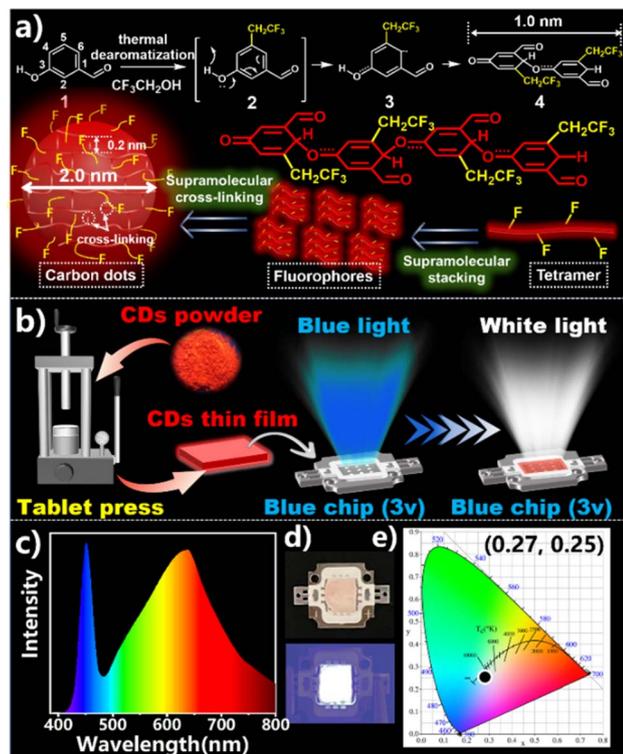
Fig. 5 (a) Mechanisms of CD formation; (b) LED production diagram; (c) corresponding emission spectra; (d) photos of LEDs; (e) CIE colour coordinates of white LEDs.

hydroxybenzaldehyde. The hydrothermal reaction that occurred when trifluoroethanol was combined with other solvents (ethanol, methanol or water) in different proportions to form the reaction solvent also confirmed that the action of F atoms led to SSF. The doping of F atoms is detrimental to the formation of CDs, such as leading to smaller particle sizes, shorter conjugated structures in the carbon nucleus, and lower fluorescence efficiency.[56] However, F atoms can enhance the interaction between carbon dots, promote their crystallization, and induce the emission of solid fluorescence, which is referred to as the crystal induced emission effect.[57]

Considering that the F-CDs exhibited strong SSF in the deep-red region, we used them to prepare a CD thin film and white light-emitting LED.[58] Due to the presence of F atoms, we expected strong interactions between molecules, so we pressed the F-CD powder into a tablet to form a film, which was subsequently covered with a blue chip to obtain a luminous white LED (Fig. 5b). As shown in Fig. 5c and d, the photoluminescence spectra of white LEDs prepared from F-CD films show panchromatic emission at 400–700 nm, where two different emission bands centred at 451 nm and 636 nm overlap each other and display (0.36, 0.37) CIE coordinates (Fig. 5e).

In summary, we proposed a simple and novel F-strategy for the synthesis of solid-state red fluorescent F-CDs. Both the FTIR and XPS data confirmed the formation of C–F bonds at the periphery/edge or on the surface of the F-CDs. The XRD data demonstrated the formation of crystalline structures in the F-

CDs. Unlike the H-CDs that contained no F dopant, the F-CDs showed bright red fluorescence in the solid state. Strong F–F interactions are vital for inducing crystallization, and solid luminescence is achieved by blocking the non-radiative energy dissipation pathways of crystalline organizations. This study provides novel evidence supporting the synthesis and application of SSF CDs.

Author contributions

Conceptualization: L. L. and X. L.; methodology: Y. L., H. S. and C. L.; writing—original draft preparation: T. G. and G. Y.; writing—review and editing: F. Y., D. H. and Y. Z. All authors have read and agreed to the published version of the manuscript.

Conflicts of interest

There are no conflicts to declare.

Acknowledgements

Notes and references

1 S. N. Baker and G. A. Baker, *Angew. Chem., Int. Ed.*, 2010, **49**, 6726–6744.

2 H. Wang, L. Ai, H. Song, Z. Song, X. Yong, S. Qu and S. Lu, *Adv. Funct. Mater.*, 2023, **35**, 2303756.

3 B. Wang and S. Lu, *Matter*, 2022, **5**, 110–149.

4 T. Feng, Q. Zeng, S. Lu, X. Yan, J. Liu, S. Tao, M. Yang and B. Yang, *ACS Photonics*, 2018, **5**, 502–510.

5 Y. Zhang, K. Liu, J. Yu, H. Chen, R. Fu, S. Zhu, Z. Chen, S. Wang and S. Lu, *Nano Res.*, 2022, **15**, 6399–6406.

6 H. Li, Y. Chen, H. Wang, H. Wang, Q. Liao, S. Han, Y. Li, D. Wang, G. Li and Y. Deng, *Adv. Funct. Mater.*, 2023, **33**, 2302862.

7 Y. Zhang, H. Song, L. Wang, J. Yu, B. Wang, Y. Hu, S. Zang, B. Yang and S. Lu, *Angew. Chem., Int. Ed.*, 2021, **60**, 25514–25521.

8 H. Yang, Y. Liu, Z. Guo, B. Lei, J. Zhuang, X. Zhang, Z. Liu and C. Hu, *Nat. Commun.*, 2019, **10**, 1789.

9 X. Ba, L. Zhang, Y. Yin, F. Jiang, P. Jiang and Y. Liu, *J. Colloid Interface Sci.*, 2020, **565**, 77–85.

10 X. Xu, L. Mo, Y. Li, X. Pan, G. Hu, B. Lei, X. Zhang, M. Zheng, J. Zhuang and Y. Liu, *Adv. Mater.*, 2021, **33**, 2104872.

11 J. Wang, J. Zheng, Y. Yang, X. Liu, J. Qiu and Y. Tian, *Carbon*, 2022, **190**, 22–31.

12 B. Xu, J. Li, J. Zhang, H. Ning, X. Fang, J. Shen, H. Zhou, T. Jiang, Z. Gao, X. Meng and Z. Wang, *Adv. Sci.*, 2023, **10**, 2205788.

13 M. Park, Y. Jeong, H. S. Kim, W. Lee, S. Nam, S. Lee, H. Yoon, J. Kim, S. Yoo and S. Jeon, *Adv. Funct. Mater.*, 2021, **31**, 2102741.

14 Y. Wang, H. Li, D. Wang and B. Z. Tang, *Adv. Funct. Mater.*, 2021, **31**, 2006952.

15 Y. An, C. Liu, M. Chen, X. Yin, D. Hou, Y. Zheng, R. Shi, X. He and X. Lin, *ACS Sustain. Chem. Eng.*, 2022, **11**, 23–28.

16 L. Ai, Z. Song, M. Nie, J. Yu, F. Liu, H. Song, B. Zhang, G. I. N. Waterhouse and S. Lu, *Angew. Chem., Int. Ed.*, 2023, **62**, 202217822.

17 Z. Wan, Y. Li, Y. Zhou, D. Peng, X. Zhang, J. Zhuang, B. Lei, Y. Liu and C. Hu, *Adv. Funct. Mater.*, 2023, **33**, 2207296.

18 J. Bai, *Inorg. Chem. Commun.*, 2023, **151**, 110614.

19 J. Tan, Q. Li, S. Meng, Y. Li, J. Yang, Y. Ye, Z. Tang, S. Qu and X. Ren, *Adv. Mater.*, 2021, **33**, 2006781.

20 Z. Zhou, E. V. Ushakova, E. Liu, X. Bao, D. Li, D. Zhou, Z. Tan, S. Qu and A. L. Rogach, *Nanoscale*, 2020, **12**, 10987–10993.

21 J. Wang, S. Zhang, Y. Li, C. Wu, W. Zhang, H. Zhang, Z. Xie and S. Zhou, *Small*, 2022, **18**, 2203152.

22 J. Liu, J. Zhang, Y. Zhou, D. Xiao, Y. Zhuo, Y. Chai and R. Yuan, *Anal. Chem.*, 2021, **93**, 10890–10897.

23 K. Chu, Z. Ding and E. Zysman-Colman, *Chem.–Eur. J.*, 2023, **29**, 202301504.

24 C. Jäckel, M. Salwiczek and B. Koksch, *Angew. Chem., Int. Ed.*, 2006, **45**, 4198–4203.

25 G. V. Janjić, S. T. Jelić, N. P. Trišović, D. M. Popović, I. S. Đorđević and M. K. Milčić, *Cryst. Growth Des.*, 2020, **20**, 2943–2951.

26 H. Omorodion, B. Twamley, J. A. Platts and R. J. Baker, *Cryst. Growth Des.*, 2015, **15**, 2835–2841.

27 G. Zuo, A. Xie, X. Pan, T. Su, J. Li and W. Dong, *ACS Appl. Nano Mater.*, 2018, **1**, 2376–2385.

28 W. Yang, H. Zhang, J. Lai, X. Peng, Y. Hu, W. Gu and L. Ye, *Carbon*, 2018, **128**, 78–85.

29 T. Li, W. Shi, Q. Mao and X. Chen, *J. Mater. Chem. C*, 2021, **9**, 17357–17364.

30 L. Zhang, M. Wu, Z. Wang, H. Guo, L. Wang and M. Wu, *ACS Sustain. Chem. Eng.*, 2021, **9**, 16262–16269.

31 P. Long, Y. Feng, C. Cao, Y. Li, J. Han, S. Li, C. Peng, Z. Li and W. Feng, *Adv. Funct. Mater.*, 2018, **28**, 1800791.

32 L. E. Zimmer, C. Sparr and R. Gilmour, *Angew. Chem., Int. Ed.*, 2011, **50**, 11860–11871.

33 B. Cheng, L. Cao, C. Li, F. Huo, Q. Meng, G. Tong, X. Wu, L. Bu, L. Rao and S. Wang, *Chin. Chem. Lett.*, 2023, **34**, 108969.

34 Y. Wang, Y. Liu, X. Hao, X. Zhou, H. Peng, Z. Shen, I. I. Smalyukh, X. Xie and B. Yang, *Adv. Mater.*, 2023, **35**, 2303680.

35 P. Long, Y. Feng, C. Cao, Y. Li, J. Han, S. Li, C. Peng, Z. Li and W. Feng, *Adv. Funct. Mater.*, 2018, **28**, 1800791.

36 J. Xu, Q. Liang, Z. Li, V. Y. Osipov, Y. Lin, B. Ge, Q. Xu, J. Zhu and H. Bi, *Adv. Mater.*, 2022, **34**, 2200011.

37 M. Zheng, H. Jia, B. Zhao, C. Zhang, Q. Dang, H. Ma, K. Xu and Z. Tan, *Small*, 2023, **19**, 2206715.

38 M. P. Han, K. Tang, Y. Wang, B. Lin and T. Cheng, *Nanoscale*, 2015, **7**, 1586–1595.

39 H. Li, Z. Zhang, J. Ding, Y. Xu, G. Chen, J. Liu, L. Zhao, N. Huang, Z. He, Y. Li and L. Ding, *Carbon*, 2019, **149**, 342–349.

40 Y. Chen, M. Zheng, Y. Xiao, H. Dong, H. Zhang, J. Zhuang, H. Hu, B. Lei and Y. Liu, *Adv. Mater.*, 2016, **28**, 312–318.

41 Y. Ding, X. Wang, M. Tang and H. Qiu, *Adv. Sci.*, 2022, **9**, 2103833.

42 H. Ding, J. Xu, L. Jiang, C. Dong, Q. Meng, S. U. Rehman, J. Wang, Z. Ge, V. Y. Osipov and H. Bi, *Chin. Chem. Lett.*, 2021, **32**, 3646–3651.

43 J. Shao, S. Zhu, H. Liu, Y. Song, S. Tao and B. Yang, *Adv. Sci.*, 2017, **4**, 1700395.

44 S. Chen, T. Han and B. Z. Tang, *Adv. Funct. Mater.*, 2023, **33**, 2307267.

45 H. Ding, S.-B. Yu, J.-S. Wei and H.-M. Xiong, *ACS Nano*, 2016, **10**, 484–491.

46 L. Jiang, H. Ding, S. Lu, T. Geng, G. Xiao, B. Zou and H. Bi, *Angew. Chem., Int. Ed.*, 2020, **59**, 9986–9991.

47 P. Long, Y. Feng, Y. Li, C. Cao, S. Li, H. An, C. Qin, J. Han and W. Feng, *ACS Appl. Mater. Interfaces*, 2017, **9**, 37981–37990.

48 F. Liu, Z. Li, Y. Li, Y. Feng and W. Feng, *Carbon*, 2021, **181**, 9–15.

49 J. Li and X. Gong, *Mater. Today Chem.*, 2022, **26**, 101255.

50 Y. Li, C. Liu, H. Sun, M. Chen, D. Hou, Y. Zheng, H. Xie, B. Zhou and X. Lin, *Adv. Sci.*, 2023, **10**, 2300543.

51 M. K. Bera, P. Pal and S. Malik, *J. Mater. Chem. C*, 2020, **8**, 788–802.

52 G. Hu, Y. Wang, S. Zhang, H. Ding, Z. Zhou, J. Wei, X. Li and H. Xiong, *Carbon*, 2014, **203**, 1–10.

53 S. Zhu, L. Wang, N. Zhou, X. Zhao, Y. Song, S. Maharjan, J. Zhang, L. Lu, H. Wang and B. Yang, *Chem. Commun.*, 2014, **50**, 13845–13848.

54 S. Zhu, Y. Song, J. Shao, X. Zhao and B. Yang, *Angew. Chem., Int. Ed.*, 2015, **54**, 14626–14637.

55 M. Ge, S. Han, Y. Ma, J. Li, S. Liu, Z. Chen and S. Li, *Adv. Opt. Mater.*, 2021, **9**, 2101092.

56 H. Song, J. Yu, Z. Tang, B. Yang and S. Lu, *Adv. Energy Mater.*, 2022, **12**, 2102573.

57 M. Yamauchi, K. Yokoyama, N. Aratani, H. Yamada and S. Masuo, *Angew. Chem., Int. Ed.*, 2019, **58**, 14173–14178.

58 C. Ji, W. Xu, Q. Han, T. Zhao, J. Deng and Z. Peng, *Nano Energy*, 2023, **114**, 108623.